

Elongation Flow Studies of DNA as a Function of Temperature

N. SASAKI, Y. MAKI, M. NAKATA

Division of Biological Sciences, Graduate School of Science, Hokkaido University, Kita-ku, Sapporo 060-0810, Japan

Received 9 November 2000; accepted 2 March 2001

ABSTRACT: The response of T4-phage DNA molecules to an elongational flow field was monitored by flow-induced birefringence as a function of temperature. The flow-induced birefringence observed in this study was localized in the pure elongational flow area with a critical strain rate, indicating that the birefringence was attributed to a coil–stretch transition of DNA molecules. The slight decrease in the birefringence intensity with increases in temperature to 40°C was explained by a thermal-activation process. At temperatures above 50°C, flow-induced birefringence decreased remarkably, and no birefringence was observed at temperatures above 60°C. After the flow experiments, ambient temperature was reduced back to room temperature, and flow experiments at room temperature were performed again. Flow-induced birefringence was recovered almost completely in samples for which the first flow measurements were made at temperatures below 53°C. Irreversible changes were observed for samples for which the first flow experiments were performed at temperatures above 55°C. The temperature dependence of UV-absorption spectra revealed that the double-strand DNA helix began to partially untwine at a temperature over 50°C, and duplexes became almost completely untwined at a temperature over 55°C. A comparison of electrophoresis patterns for untwined molecules showed that flow-induced scission of DNA molecules occurred in a sample solution in flow experiments performed at 65°C, while no molecular weight reduction was observed in the sample solution at 55°C. In this article, this difference between the untwined DNA molecules is discussed on the basis of the thermally activated bond scission (TABS) model. © 2002 John Wiley & Sons, Inc. *J Appl Polym Sci* 83: 1357–1365, 2002

Key words: elongational flow; DNA molecules; flow-induced birefringence; flow-induced scission

INTRODUCTION

DNA molecules of phage origin, such as T4-phage DNA, T7-phage DNA, and λ -phage DNA, have contour lengths over several tens of microns in

their double-strand state. DNA molecules of that size are observable using optical microscopes in conjunction with a fluorescent micrographic method.^{1–4} In a sodium chloride aqueous solution of a certain concentration, since the persistence length of a phage DNA molecule ranges from 50 to 90 nm,^{5,6} DNA molecules even in a double-strand state have been considered to be a model of semiflexible coil or wormlike chains.^{5,7} Thermal denaturation of DNA molecules has been regarded as a process of a helix–coil transition.⁸ However, because a DNA molecule in a helix structure is regarded as a semiflexible random coil, the helix–

Correspondence to: N. Sasaki.
Contract grant sponsor: Suhara Memorial Foundation.
Contract grant sponsor: Ministry of Education, Culture, Science, and Sports of Japan; contract grant number: 08455447.

Journal of Applied Polymer Science, Vol. 83, 1357–1365 (2002)
© 2002 John Wiley & Sons, Inc.
DOI 10.1002/app.10015

coil transition of a DNA molecule is thought to be hydrodynamically different from that of an α -helical polypeptide chain.

The hydrodynamic response of a chain molecule to an elongational flow field provides various quantities characterizing chain properties such as flexibility.⁹ To monitor the response of polymers to the elongational flow field, a flow birefringence technique has been employed. On the basis of accumulated results, it is possible to classify polymers by the flow-induced birefringence pattern. For flexible polymers, elongational flow-induced birefringence is localized along the pure elongational flow field. In a birefringence (Δn) versus elongational strain rate $\dot{\epsilon}$ plot, there is a critical strain rate $\dot{\epsilon}_c$ below which no birefringence is observed, and Δn increases rapidly over this strain rate. This phenomenon has been rationalized as a coil–stretch transition of flexible polymer chains.¹⁰ In the case of rigid-rodlike molecules, nonlocalized birefringence is observed over the whole irradiated field around the pure elongational flow field.^{11,12} Δn increases continuously with $\dot{\epsilon}$ and there is no critical strain rate. By making use of these differences in the response of polymers to the elongational flow field, conformational transitions of biopolymers have been successfully investigated.^{13–16} The elongational flow field has been shown to be a new useful tool for studying the conformational transition of both synthetic and biological polymers. Results from hydrodynamic studies have contributed to an understanding of the global properties of macromolecules.

The aim of the present study was to determine the hydrodynamic features of thermal denaturation of long DNA molecules. For this purpose, the response of DNA molecules to an elongational flow field was observed as a function of temperature using a flow birefringence technique. In this article, the results obtained from flow experiments are discussed in terms of change in the molecular conformation by thermal untwining and a scission of DNA molecules by the elongational flow field.

EXPERIMENTAL

Materials

We used coliphage T4 DNA, whose molecular weight is 1.1×10^8 Da, that is, 167,000 base pairs.

T4 DNA molecules in a solution of 10 mM Tris–HCl, pH 8.0, and 1.0 mM EDTA were purchased from the Sigma Chemical Co. (St. Louis, MO). DNA solutions were prepared by dilution with water containing 0.2M NaCl. For the elongational flow measurements, 90% (v/v) of glycerol was added as a viscosity builder. The final concentration of DNA was 5 $\mu\text{g}/\text{mL}$. T4 DNA molecules have been reported to have a radius of gyration (R_g) of about 1 μm in an aqueous solution.⁶ This R_g value indicates that the critical concentration c^* for a dilute solution of T4 DNA should be 12.9 $\mu\text{g}/\text{mL}$, which means that the concentration of all samples examined in this work was below c^* .

Apparatus and Method

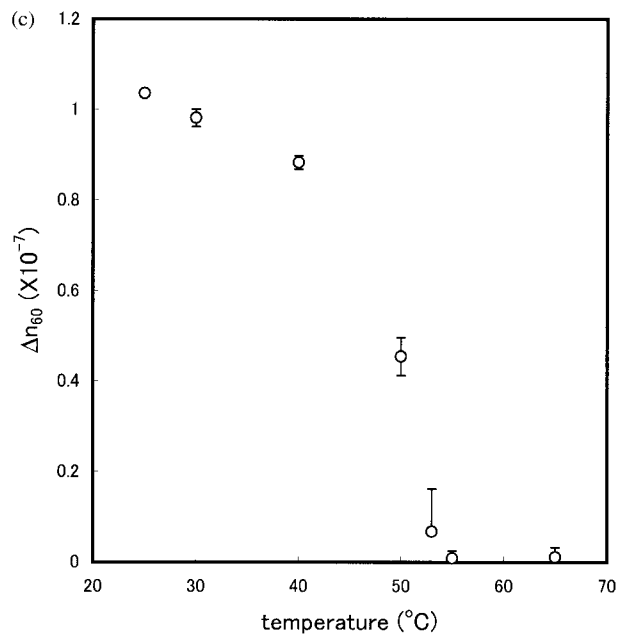
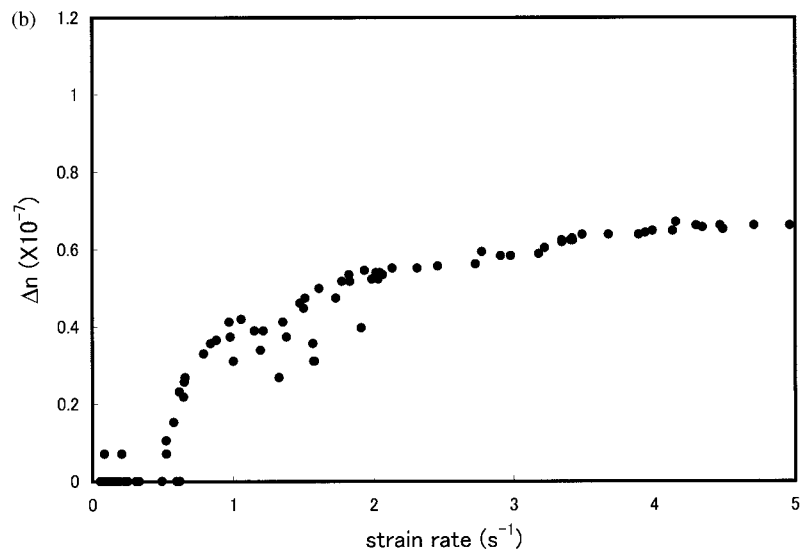
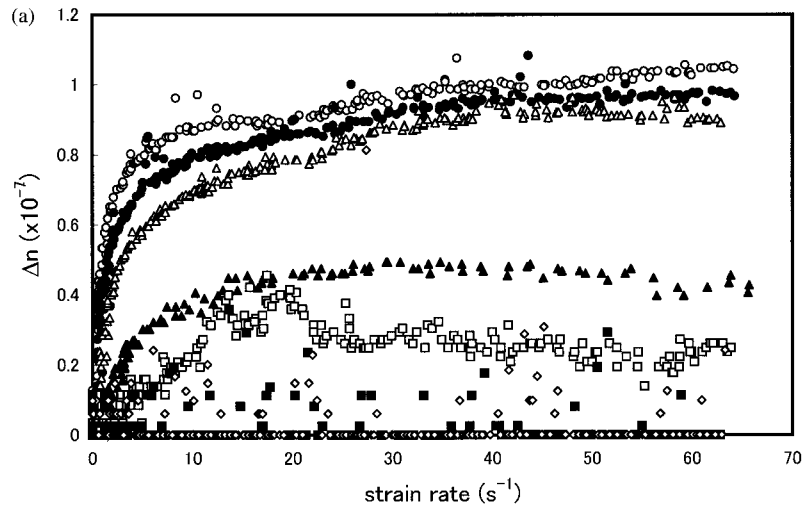
The elongational flow field was generated by a four-roller mill system, originally utilized by Taylor for the study of liquid droplets in a flow field.¹⁷ Details of the four-roller mill used in this study were described elsewhere.¹⁶ To quantify the response of DNA molecules to the elongational flow field, the flow-induced birefringence, Δn , generated in the DNA solution was observed. Measurements of Δn as a function of the elongational strain rate, $\dot{\epsilon}$, were performed isothermally over the range of $\dot{\epsilon} = 0\text{--}70 \text{ s}^{-1}$. The elongational strain-rate value was determined by Torza's formula for a four-roller mill apparatus.¹⁸ The temperature of the solution was changed from 25 to 65°C. At each temperature, the temperature was kept within $\pm 1^\circ\text{C}$ from the nominal value by the use of a heat jacket through which thermally regulated water was circulated. By observing the UV spectrum around 260 nm, using a SHIMADZU UV-160A spectrometer, the thermal denaturation of DNA at each temperature was assessed. Degradation of DNA molecules was investigated using agarose gel electrophoresis.

RESULTS AND DISCUSSION

Elongational Flow-induced Birefringence

Figure 1(a) shows the flow birefringence, Δn , plotted against the elongational strain rate, $\dot{\epsilon}$, at temperatures from 25 to 65°C. The birefringence ob-

Figure 1 (a) Flow-induced birefringence Δn plotted against the elongational strain rate $\dot{\epsilon}$ at (○) 25.0°C, (●) 30.0°C, (△) 40.0°C, (▲) 50.0°C, (□) 53.0°C, (■) 55.0°C, and (◇) 65.0°C. (b) Magnification of the initial part of Δn versus $\dot{\epsilon}$ plot for 30.0°C. (c) Δn at $\dot{\epsilon} = 50 \text{ s}^{-1}$ plotted against temperature.



served was localized along the pure elongational flow field and had a critical strain rate, $\dot{\epsilon}_c$, in the strain-rate dependence as shown in Figure 1(b). These results indicate a typical coil–stretch transition phenomenon, although the Δn versus $\dot{\epsilon}$ curve at about $\dot{\epsilon}_c$ has less criticality compared with the coil–stretch transition of a typical flexible polymer. The birefringence originated from the coil–stretch transition of double-strand DNA molecules. The reduction in criticality has been explained by the free-draining nature of DNA molecules.¹⁹ The Δn value became saturated at about $\dot{\epsilon} \sim 50 \text{ s}^{-1}$. Figure 1(c) shows the temperature dependence of Δn at 60 s^{-1} . The Δn value gradually decreases up to 40°C and decreased rapidly over 50°C , and no birefringence was observed at temperatures above 55°C . Figure 2(a) shows the critical strain rate, $\dot{\epsilon}_c$, at which the coil–stretch transition is expected to occur, as a function of temperature. Over 50°C , $\dot{\epsilon}_c$ increased rapidly with the temperature. Elongation of a polymer chain occurs at the strain rate where the frictional drag force by solvent molecules overcomes the entropic retraction force of the polymer chain. As the solvent viscosity changes with the temperature, the critical strain rate will also change with the temperature. Figure 2(b) shows an Arrhenius plot of $\dot{\epsilon}_c$ against the inverse of absolute temperature. From room temperature to 40°C , there is a linear relation, and over 50°C , data points deflect from the linear relation. The linear relation in $\dot{\epsilon}_c$ and $1/T$ indicates that the activation energy for the coil–stretching process does not change within the temperature range in which a linear relation holds. Therefore, it is concluded that the hydrodynamic shape of the DNA molecule remained unchanged in the temperature range to 40°C . Figure 3 shows Δn plotted against the reduced strain rate:

$$\dot{\epsilon}_R = (\dot{\epsilon} - \dot{\epsilon}_c)/\dot{\epsilon}_c = (\dot{\epsilon}/\dot{\epsilon}_c) - 1 \quad (1)$$

where the first term on the right-hand side indicates the Deborah number. By plotting Δn against $\dot{\epsilon}_R$, it is possible to compare the stretching processes of polymer chains with different values of $\dot{\epsilon}_c$.²⁰ Δn versus $\dot{\epsilon}_R$ curves for data obtained at 25, 30, and 40°C were superimposed on each other, and a single master curve was obtained, while those for data obtained at temperatures over 50°C were deflected from the master curve. These results also indicate that the hydrodynamic properties of DNA molecules at tempera-

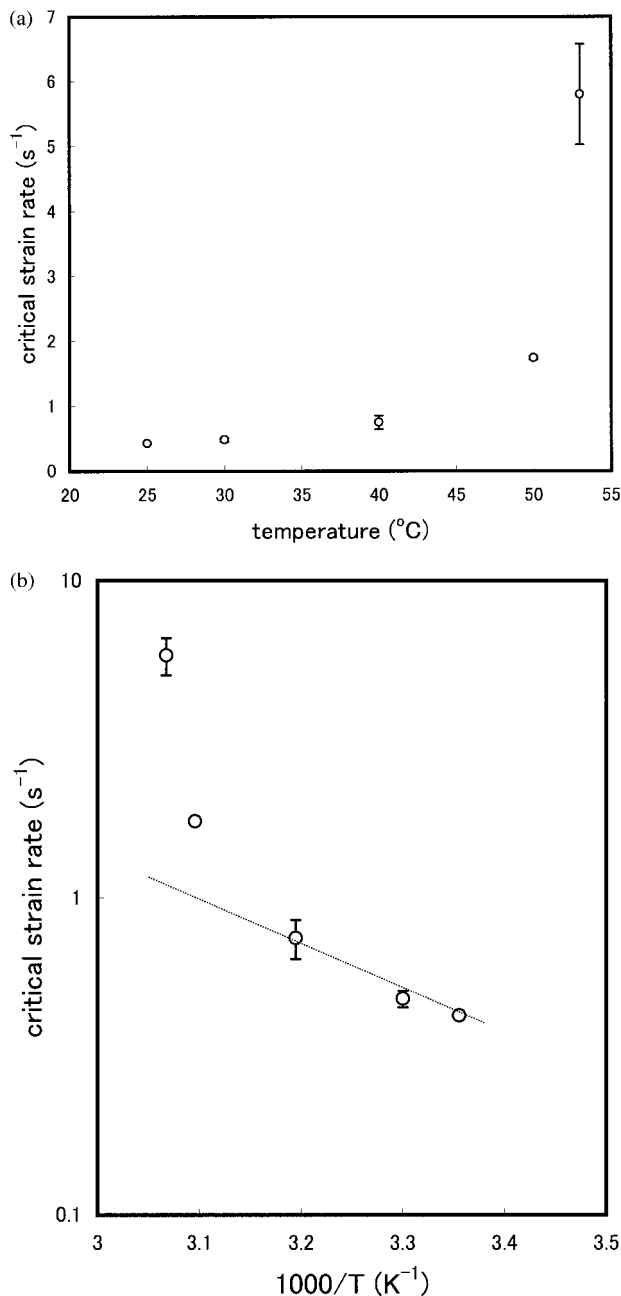


Figure 2 (a) Critical strain rate $\dot{\epsilon}_c$ plotted against temperature. (b) Arrhenius plot of $\dot{\epsilon}_c$.

tures over 50°C are different from those at temperatures in the range of 25 – 40°C .

Figure 4 shows values of Δn measured at 60 s^{-1} as a function of temperature (\circ). Filled circles (\bullet) are Δn values measured at 25°C and 60 s^{-1} after the first flow experiments at the indicated temperatures. The second flow measurements at 25°C were performed at 30 min after the solution temperature had been reduced to 25°C . To 53°C ,

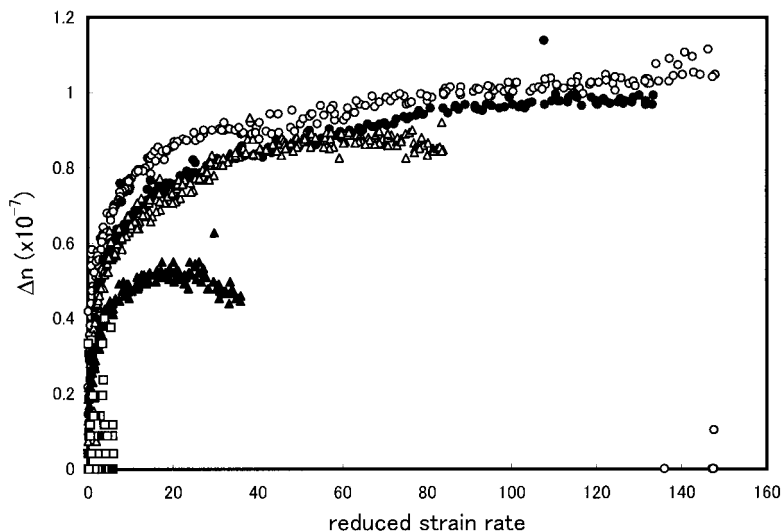


Figure 3 Δn plotted against reduced strain rate, $\dot{\epsilon}_R = (\dot{\epsilon} - \dot{\epsilon}_c)/\dot{\epsilon}_c$, for different temperatures. Symbols for each temperature are the same as those in Figure 1(a).

Δn values for the second flow experiments almost completely recovered at room temperature but recovered only partially at 55°C. Over 65°C, no birefringence was observed in either the first or second experiment.

UV Spectroscopic Results

Figure 5 shows the temperature dependence of UV absorption at 260 nm for the same DNA so-

lution as that used for the elongational flow experiments. Partial untwining of a DNA duplex occurs at temperatures over 50°C. The observed untwining temperature is slightly lower than those reported in the literature. The DNA solution tested contained 90% glycerol. Although its activity is not so high, glycerol is listed as one of the denaturing agents of DNA molecules.²¹ Therefore, the difference in untwining tempera-

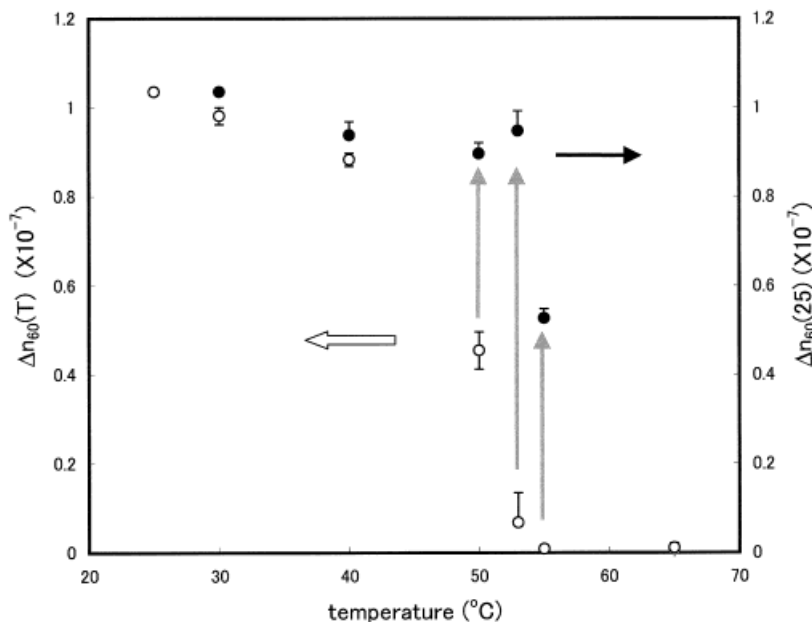


Figure 4 (○) Δn measured at $\dot{\epsilon} = 60 \text{ s}^{-1}$ plotted against temperature. (●) Δn values were measured at 25.0°C and 60 s^{-1} , after the first flow experiments at each temperature.

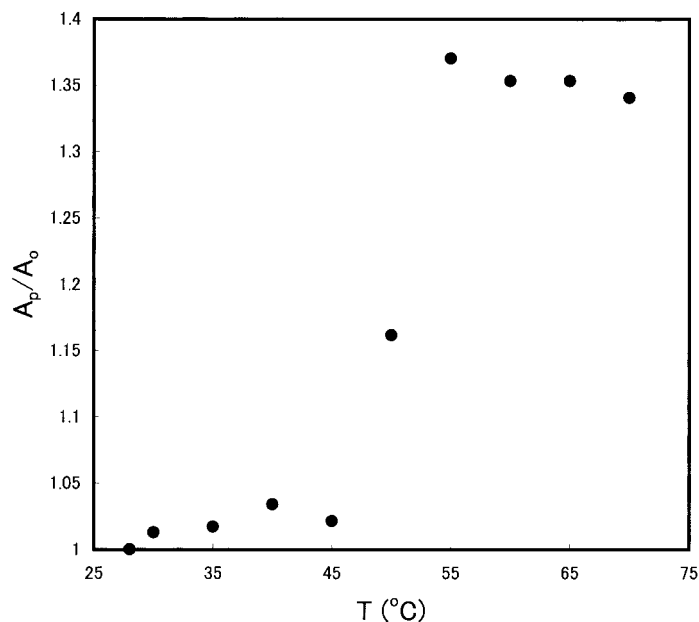


Figure 5 UV absorption at 260 nm of DNA sample solution used for the flow experiments plotted against temperature.

tures was attributed to the glycerol in the solution used in the present study. The DNA chains in the untwining part would be random-coil-like chains and would not contribute to the flow-induced birefringence unless the single-strand chains were considerably stretched. This is why the birefringence at temperatures over 50°C was smaller than that observed at 25–40°C. According to Figure 4, in DNA molecules at temperatures of 50 and 53°C, the untwining region almost completely recovered its initial double-stranded structure after the solution was cooled to 25°C. By thermal untwining, it seems that the resistance of DNA molecules against the stretching force increases, according to the deflection of ϵ_c from the Arrhenius law and the rapid increase with increases in temperature thereafter [Fig. 2(b)]. Single-strand DNA molecules are more flexible than are DNA duplexes, suggesting that the entropic contraction force of untwined chains is larger than that of double-strand DNA molecules.

Electrophoresis and Elongational Flow Field-induced Scission of DNA Molecules

Figure 6 shows electrophoresis bands of DNA solutions after the flow experiments at indicated temperatures. Although seen only slightly, but clearly, the band of 55°C is found to be located at lower molecular weight than that of 25°C. At 65°C, the electrophoresis band shifted also in the

direction of lower molecular weight, and at the same time, the bandwidth increased. In our previous investigation, at room temperature, no deg-

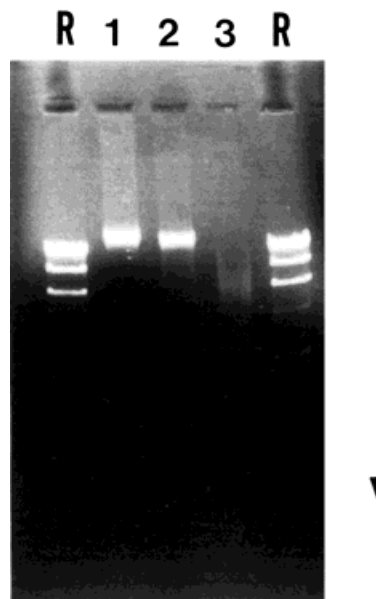


Figure 6 Agarose gel electrophoresis of T4 DNA sample solutions after the flow experiments. Lanes 1, 2, and 3 show the patterns for sample solutions after flow experiments performed at 25, 55, and 65°C, respectively. Lane R shows a set of monodisperse calibrant markers. The arrow indicates the direction of migration, that is, decreasing molecular weight.

Table I Molecular Weight Corresponding to the Electrophoresis Bands

Lane	Molecular Weight (Da)
25°C ^a	1.1×10^8
55°C	6.0×10^7
65°C	4.7×10^6

^a Used as a reference.

radiation of the molecular weight of T4-phage DNA was observed at the strain rate up to 176 s^{-1} after more than 100 passes.¹⁶ Then, the 25°C band can be regarded as indicating the molecular weight of intact T4 DNA. Using the 25°C band as the reference with the reference bands in the R lanes, molecular weights of the shifted bands were estimated and are listed in Table I. The molecular weight value corresponding to the 55°C band was almost half of that for the intact T4-phage DNA. The center of the shifted and broadened band at 65°C is located at almost 1/24 times that of the intact T4-phage DNA. These features of the 55 and 65°C bands suggest that molecular scission caused by the flow occurs at these temperatures.

It is well known that scission of polymers can occur in flow fields where the mechanical forces associated with the flow field are sufficient to rupture the covalent bonds along the chain. A number of fracture studies have been performed, and the results have been rationalized within a theoretical framework known as the thermally activated barrier to scission (TABS) model.^{22–25} According to the TABS model, fracture proceeds in an elongational flow field as a two-stage process. In the first stage, molecules are stretched by the elongational flow field into an extended conformation and are aligned with their molecular axes parallel to the flow direction. In the second stage, the extended conformation is then subjected to fracture. Scission of the extended conformation always occurs near the midpoint, where the stress in the molecule reaches a maximum value, in accordance with the theoretical prediction of Frenkel.²⁶ Regarding the results shown in Figure 6, it is not unreasonable to investigate the scission that occurred at 55°C on the basis of the TABS model.

Fracture studies on DNA molecules have also been performed, and the results have been analyzed using the TABS model.²⁷ For λ -phage DNA, the fracture strain rate, $\dot{\epsilon}_f^\lambda$, was determined to be

$6.8 \times 10^3 \text{ s}^{-1}$. This value is two orders of magnitude larger than our uppermost strain rate (70 s^{-1}). According to the TABS model, the critical strain rate for fracture is related to the contour length, L , and then to the molecular weight, M_w , of a polymer chain by the relationship²²

$$\dot{\epsilon}_f \propto 1/L^2 = 1/M_w^2 \quad (2)$$

On the basis of this equation, the critical fracture strain rate for T4-phage DNA $\dot{\epsilon}_f^{\text{T4}}$ was estimated as follows: Since the molecular weight of λ -phage DNA and T4-phage DNA are 31.5 and 110 MDa, respectively,

$$\dot{\epsilon}_f^\lambda / \dot{\epsilon}_f^{\text{T4}} = [(31.5/2)/110]^{-2} \quad (3)$$

where 1/2 in the numerator indicates that λ -phage DNA is circular. Using the value $\dot{\epsilon}_f^\lambda = 6.8 \times 10^3 \text{ s}^{-1}$, $\dot{\epsilon}_f^{\text{T4}}$ was determined to be 139 s^{-1} . As mentioned above, for T4 DNA, no molecular weight degradation was observed at the strain rate after more than 100 passes.¹⁶ The scission of circular λ -phage DNA may be somewhat different from that of linear DNA molecules. It has been reported that no degradation of T7-phage DNA ($M_w = 25 \text{ MDa}$) occurred after 40 passes at the strain rate at $12,000 \text{ s}^{-1}$, that is, $\dot{\epsilon}_f^{\text{T7}} > 12,000 \text{ s}^{-1}$.²⁷ By the same procedure using eqs. (2) and (3), the lower limit of $\dot{\epsilon}_f^{\text{T4}}$ was estimated to be $\dot{\epsilon}_f^{\text{T4}} > 620 \text{ s}^{-1}$. Although the expected value for T4-phage DNA was much smaller than that for λ -phage DNA and for T7-phage DNA, the value is larger than the uppermost strain rate of our apparatus (70 s^{-1}), up to which untwined DNA molecules were fractured. DNA molecules in these discussions were in a double-stranded state. In Figure 5, the conformational transition seems to have been completed at 55°C, that is, the DNA molecule is thought to have been almost completely untwined. This suggests that untwined DNA molecules are not so stable against fracture caused by the flow field compared with double-strand DNA molecules.

In Figure 6, flow-induced scission was also observed in the samples used for the flow experiments at 65°C. But, as compared with the result for 55°C, the estimated molecular weight was much smaller than that of intact T4 DNA and the band was much broader. This indicates that the scission rate drastically increased with increasing temperature. According to the TABS model, the scission rate, $K(T)$, is described as

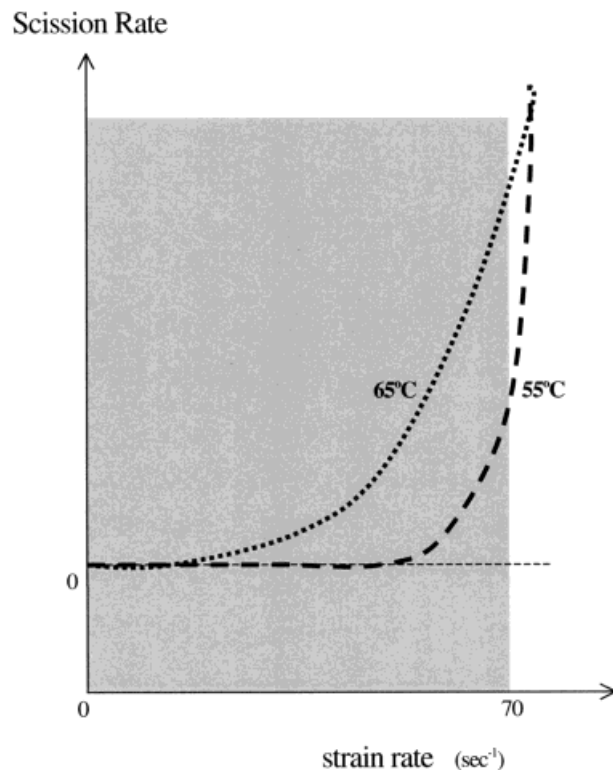


Figure 7 Schematic drawing of the temperature effect on the flow-induced fracture rate. At a strain rate $\dot{\epsilon}$ slightly smaller than $\dot{\epsilon}_f$, the fracture rate increases as a result of broadening of the foot in $K(t)$ versus $\dot{\epsilon}$ plot with increase in temperature. The four-roll mill used in this study covers the gray-colored strain-rate region.

$$K(T) = A \exp[-u_0(\dot{\epsilon})/k_B T] \quad (4)$$

$$u_0 = U_0 - (Ca\eta_s l^2 N^2 \dot{\epsilon} / 8) \quad (5)$$

where U_0 is the dissociation energy; C , the correction factor determined by the molecular shape; a , the stretched bond length; η_s , the solvent viscosity; l , the monomer length; and N , the number of monomers.²³ A is the preexponential factor regarded as the attempt frequency for fracture and the scission rate at $\dot{\epsilon} = \dot{\epsilon}_f$. If experiments are performed at $\dot{\epsilon} \leq \dot{\epsilon}_f$, $u'_0(\dot{\epsilon}) > 0$, then $K(T)$ would change with the temperature according to the usual Arrhenius law. Equation (4) suggests that the scission rate can increase with an increase in temperature. Figure 7 shows $K(T)$ schematically plotted against the strain rate at different temperatures. At a strain rate smaller than $\dot{\epsilon}_f$, even $K(T) \sim 0$ at T_0 , at $T(>T_0)$, $K(T)$ could have a definite value. The developed foot of the $K(T)$ versus $\dot{\epsilon}$ plot slightly below $\dot{\epsilon}_f$ with an increase in

temperature can explain the difference in flow behaviors of untwined DNA molecules at 55 and 65°C. The difference suggests that $\dot{\epsilon}_f$ for untwined T4 DNA molecules is larger than 70 s^{-1} .

CONCLUSIONS

By monitoring the elongational flow-induced birefringence, the hydrodynamic features of the thermal denaturation process of T4-phage DNA molecules were investigated. A remarkable reduction in birefringence was observed at about 50°C, and no birefringence was observed at temperatures above 65°C. With the aid of UV spectra, these changes corresponded to thermal untwining of a DNA duplex. At temperatures to 50°C, the change was reversible, while at temperatures above 65°C, the birefringence reduction was not recovered by cooling the solution to 25°C. This irreversible change was attributed to the flow-induced scission of DNA molecules. Untwined DNA molecules are much more unstable compared with a DNA duplex, probably because of the disappearance of the structural stability factor by untwining.

We are grateful for the financial support from the Suhara Memorial Foundation and a Grant-in-Aid for Scientific Research (No. 08455447) from the Ministry of Education, Culture, Science, and Sports of Japan.

REFERENCES

1. Matsumoto, S.; Morikawa, K.; Yanagida, M. *J Mol Biol* 1981, 152, 501–516.
2. Minagawa, K.; Matsuzawa, Y.; Yoshikawa, K.; Khokhlov, A. R.; Doi, M. *Biopolymers* 1994, 34, 555–558.
3. Smith, D. E.; Chu, S. *Science* 1998, 281, 1335–1340.
4. Wakabayashi, K.; Sasaki, N.; Hikichi, K. *J Appl Polym Sci* 2000, 76, 1351–1358.
5. Hays, J. B.; Mager, M. E.; Zimm, B. H. *Biopolymers* 1969, 8, 531–536.
6. Yanagida, M.; Hiraoka, Y.; Katsura, I. *Cold Spring Harbor Symp Quant Biol* 1983, 47, 177–187.
7. Perkins, T. T.; Smith, D. E.; Chu, S. *Science* 1994, 264, 819–822.
8. Zimm, B. H. *J Chem Phys* 1960, 33, 1349–1356.
9. Keller, A.; Odell, J. A. *Colloid Polym Sci* 1985, 263, 181–201.
10. De Gennes, P. G. *J Chem Phys* 1974, 60, 5030–5042.

11. Odell, J. A.; Keller, A.; Atkins, E. D. T. *Macromolecules* 1985, 18, 1443–1453.
12. Pope, D. P.; Keller, A. *Colloid Polym Sci* 1977, 255, 633–643.
13. Sasaki, N.; Atkins, E. D. T.; Fulton, S. W. *J Appl Polym Sci* 1991, 42, 2975–2985.
14. Hayakawa, I.; Sasaki, N.; Hikichi, K. *J Appl Polym Sci* 1995, 56, 661–665.
15. Hayakawa, I.; Hayashi, C.; Sasaki, N.; Hikichi, K. *J Appl Polym Sci* 1996, 61, 1731–1735.
16. Hayakawa, I.; Sasaki, N.; Hikichi, K. *Polymer* 1998, 39, 1393–1397.
17. Taylor, G. I. *Proc R Soc Lond* 1934, 146, 501–523.
18. Torza, S. J. *J Polym Sci Polym Phys Ed* 1975, 13, 43–57.
19. Odell, J. A.; Tayler, M. A. *Biopolymers* 1994, 34, 1483–1493.
20. Fujii, S.; Sasaki, N.; Nakata, M. *J Polym Sci Part B: Polym Phys* 2001, 39, 1976–1986.
21. Levine, L.; Gordon, J. A.; Jencks, W. *Biochemistry* 1963, 2, 168–175.
22. Odell, J. A.; Keller, A. *J Polym Sci Polym Phys Ed* 1986, 24, 1889–1916.
23. Odell, J. A.; Keller, A.; Rabin, Y. *J Chem Phys* 1988, 88, 4022–4028.
24. Odell, J. A.; Muller, A. J.; Narh, K. A.; Keller, A. *Macromolecules* 1990, 23, 3092–3103.
25. Narh, K. A.; Odell, J. A.; Muller, A. J.; Keller, A. *Polym Commun* 1990, 31, 2–5.
26. Frenkel, J. *Acta Physicochim URSS* 1944, 19, 51–76.
27. Atkins, E. D. T.; Tayler, M. A. *Biopolymers* 1992, 32, 911–923.